PROF. BENZHI CAI (Orcid ID : 0000-0001-8732-6465)

Article type : Original Manuscript

Melatonin protects bone marrow mesenchymal stem cells against iron overload-induced osteogenic differentiation dysfunction and senescence

Fan Yang[2*] | Lei Yang[1*] | Yuan Li[2*] | Gege Yan[2] | Chao Feng[2] | Tianyi Liu[2] | Rui Gong[2] | Ye Yuan[2,3] | Ning Wang[2] | Elina Idiiatullina[4,5] | Timur Bikkuzin[4,5] | Valentin Pavlov[5] | Yang Li[6] | Chaorun Dong[4] | Dawei Wang[1] | Yang Cao[1] | Zhenbo Han[2] | Lai Zhang[2] | Qi Huang[2] | Fengzhi Ding[2] | Zhengang Bi[1] | Benzhi Cai[2,3,4]

[1]Department of Orthopedics, The First Affiliated Hospital of Harbin Medical University, Harbin, 150001, China

[2]Department of Pharmacology (The State-Province Key Laboratories of Biomedicine-Pharmaceutics of China), College of Pharmacy, Harbin Medical University, Harbin, 150086, China

[3]Department of Clinical Pharmacy, The Affiliated Second Hospital of Harbin Medical University, Harbin, 150086, China

[4]The Northern Medicine Translational Center, Heilongjiang Province Academy of Medical Science, Harbin, 150081, China

[5]Central Laboratory of Scientific Research, Bashkir State Medical University, Ufa, 450008, Russia

[6]Center for Endemic Disease Control, Chinese Center for Disease Control and Prevention, Key Lab of Etiology and Epidemiology, Education Bureau of Heilongjiang Province & Ministry of Health, Harbin Medical University, Harbin, 150081, China

Correspondence

Prof. Lei Yang, Department of Orthopedics, The First Affiliated Hospital of Harbin Medical University, Harbin 150001, China; or Benzhi Cai, Department of Pharmacology, College of Pharmacy, Harbin Medical University, and Department of Clinical Pharmacy, The Affiliated Second Hospital of Harbin Medical University, Harbin 150086, China

E-mail: yangray83@vip.qq.com; caibenzhi@163.com

Tel: 86 451 86671354

Fax: 86 451 86671354

[*]With equal contribution to this work.

Abstract

Bone marrow mesenchymal stem cells (BMSCs) are an expandable population of stem cells which can differentiate into osteoblasts, chondrocytes and adipocytes. Dysfunction of BMSCs in response to pathological stimuli contributes to bone diseases. Melatonin, a hormone secreted from pineal gland, has been proved to be an important mediator in bone formation and mineralization. The aim of this study was to investigate whether melatonin protected against iron overload-induced dysfunction of BMSCs and its underlying mechanisms. Here, we found that iron overload induced by ferric ammonium citrate (FAC)

caused irregularly morphological changes and markedly reduced the viability in BMSCs. Consistently, osteogenic differentiation of BMSCs was significantly inhibited by iron overload, but melatonin treatment rescued osteogenic differentiation of BMSCs. Furthermore, exposure to FAC led to the senescence in BMSCs, which was attenuated by melatonin as well. Meanwhile, melatonin was able to counter the reduction of cell proliferation by iron overload in BMSCs. In addition, protective effects of melatonin on iron overload-induced dysfunction of BMSCs were abolished by its inhibitor luzindole. Also, melatonin protected BMSCs against iron overload-induced accumulation of intracellular and mitochondrial ROS level, and membrane potential depolarization. Further study uncovered that melatonin reversed the upregulation of p53, ERK and p38 protein expressions in BMSCs with iron overload. Collectively, melatonin plays a protective role in iron overload induced osteogenic differentiation dysfunction and senescence through blocking ROS accumulation and p53/ERK/p38 activation.

KEYWORDS

melatonin, bone marrow mesenchymal stem cells, iron overload, differentiation, senescence.

1 | INTRODUCTION

Bone marrow mesenchymal stem cells (BMSCs) are an expandable population of stem cells with the capability of self-renewal, and they have a latent capacity to differentiate into a variety of cell types, such as osteoblasts, chondrocytes and adipocytes.[1] BMSCs are emerging as a useful model for developmental biology and have great therapeutic potential in cell therapy and tissue regeneration.[2] Previous reports showed that BMSCs have been widely

used in the regeneration of damaged tissues, including heart, kidney and bone.[3,4] By far, multiple studies have confirmed the great potential of BMSCs in promoting regeneration of bone defects both in animal models and human.[5,6] BMSCs in vitro bone differentiation results from the activation of some well-known molecular signaling pathways, such as mitogen-activated protein kinase (MAPK) signaling pathway, Wnt/beta-catenin signaling pathway, TGF-beta/Smad and BMP signaling pathways. In addition, some osteoblast-specific signal proteins and osteoblast-specific transcription factors, including Runx2, Osterix and BMP4, also have been proved to play an important role in the osteogenic differentiation of BMSCs.[4,7-9] Besides, substantial evidence shows that the inhibited expressions of adipogenic differentiation transcriptional regulators, such as peroxisome proliferator-activated receptor γ (PPARγ) and CCAAT/enhancer binding protein (C/EBP), could promote the osteogenic differentiation of BMSCs.[9] Many studies have already demonstrated that the disruption of the balance between osteogenesis and adipogenesis of BMSCs leads to disorders such as osteoporosis.[10] Therefore, it is vital to maintain the bone homeostasis by controlling the balance of these processes during BMSCs differentiation.

Iron is an essential metal for hemoglobin synthesis and some vital enzymatic functions. Iron homeostasis is important for physiological growth and the survival of tissues and organs, and iron imbalance contributes to a variety of diseases.[11] Iron deficiency leads to anemia and sometimes organ dysfunction, on the contrary, excess iron could deposit in the tissues and ultimately lead to the pathological alteration of visceral organs.[12-14] Growing evidence indicates that iron overload in mice results in increased bone resorption and oxidative stress, leading to the changes in bone microarchitecture and bone loss.[15] Also, iron is involved in the

development of osteoporosis as well as in diseases characterized by iron overload, such as thalassemias and hemochromatosis.[16,17]

The pineal gland hormone melatonin (N-acetyl-5-methoxytryptamine) has been shown to play an important role in many physiological systems, including controlling sleep-wake rhythms, regulation of circadian cycle, cardiovascular function, immune defense, renal function, detoxification, as well as bone metabolism.[18-20] In addition to these functions, numerous studies also demonstrated that melatonin can serve as one of the most powerful endogenous antioxidant agents by direct and indirect ways.[21] It has been reported that melatonin exerted antioxidative function directly via scavenging reactive oxygen species (ROS) such as the carbonate radical, which may be involved in mitochondrial damage.[21] Furthermore, melatonin easily enters mitochondria and exerts a direct beneficial effect on the maintenance of mitochondrial homeostasis.[22] On the other hand, melatonin exerts antioxidative function indirectly by stimulating certain kinds of antioxidative enzymes, such as superoxide dismutase and catalase. The strong antioxidant properties made melatonin a promising candidate for treating and preventing a variety of diseases including cancer, neurodegenerative diseases, diabetes and bone related diseases, with oxidative stress being a major factor involved in the pathogenesis of these disorders.[23-27]

Several lines of evidence suggest that melatonin is an important regulator of precursor cell commitment and plays an important role in promoting osteogenic differentiation in MC3T3-E1 preosteoblasts, human bone cells, human osteoblasts, and BMSCs.[28,29] Moreover, increasing evidence has indicated that melatonin treatment effectively prevented osteoporosis in ovariectomized rats and increased the volume of newly formed cortical bone of femora,

promoted bone formation and prevented bone loss in perimenopausal women without major side effects.[30] In addition, melatonin exerts an osteoinductive effect by promoting osteogenic maturation of human adult mesenchymal stem cells as well as cartilage matrix synthesis by articular chondrocytes.[31]

However, whether melatonin treatment can protect BMSCs against the iron overload induced damage, as well as the underlying mechanisms remains unknown. Therefore, the aim of the present study is to characterize the pharmacological effects of melatonin, and to evaluate whether melatonin treatment could antagonize the iron overload induced dysfunction of BMSCs.

2 | MATERIALS AND METHODS

2.1 | Animals

Male C57BL/6J mice (18-20 g) were purchased from the Experimental Animal Center of Harbin Medical University. All animal protocol was approved by the Guide for the Care and Use of Laboratory Animals published by the US National Institute of Health. Additionally, all experimental procedures were carried out in strict accordance with the ethic committee of Harbin Medical University.

2.2 | Reagents

Melatonin, ferric ammonium citrate (FAC), Iron-Dextran solution, luzindole (a novel melatonin receptor antagonist) and dimethyl sulfoxide (DMSO) were all purchased from Sigma-Aldrich (St. Louis, Mo, USA). Melatonin, FAC and luzindole were dissolved in DMSO, and the final culture concentration of DMSO was ≤0.5%. Mouse Mesenchymal Stem

Cell Growth Medium (HUXMA-9011), Mesenchymal Stem Cell Osteogenic Differentiation Medium (GUXMX-90021) and Mesenchymal Stem Cell Adipogenic Differentiation Medium (GUXMX-90031) were all purchased from Cyagen (Cyagen Biosciences Inc, China). In Cell-Light EdU Apollo567 in Vitro Kits were purchased from Ribobio (Ribobio, Guangzhou, China). Cell-Counting Kit-8 (CCK-8) proliferation assay kits, β-gal staining kit, 4', 6'-diamino-2'-phenylindole (DAPI) staining solution and Reactive Oxygen Species Assay Kit were purchased from Beyotime (Beyotime Biotechnology, China). MitoSOX™ Red mitochondrial superoxide indicator was purchased from Invitrogen (Invitrogen Detection Technologies, USA). JC-1 Mitochondrial Membrane Potential Assay Kit was purchased from Abcam (Abcam, UK). qRT-PCR primers were purchased from Invitrogen (Invitrogen, Carlsbad, USA). Alkaline phosphatase, alizarin red S, and oil red O were purchased from Sigma (St, Louis. Mo. USA).

2.3 | Isolation and culture of BMSCs

The isolation and culture of BMSCs from C57BL/6J mice was approved by the Ethics Committee of Harbin Medical University. The protocol was described previously.[32] In brief, after anesthetization with an overdose of amytal sodium, the bilateral femurs and tibias were aseptically excised with removing the connective tissues around the bones. After muscles and connective tissues were further trimmed and cleaned, the epiphyses of femurs and tibias were removed to expose the marrow cavity, and the marrow was flushed out using BMSCs culture medium (HUXMA-9011) until the bones become pale. The culture medium used to flush containing BMSCs was collected, eliminating the thrombus, seeded into 25 cm^2 flasks, and cultured at 37°C in a humidified atmosphere with 95% air and 5% CO_2. BMSCs were

adherent to the bottom of the flasks due to their adherence characteristic. After 72 h, adherent cells were thoroughly washed twice with culture medium, and nonadherent cells were washed out from the flasks by changing culture medium. The medium was replaced every 3 days, during which nonadherent cells were discarded. After 7-10 days culture, when the cells reached 80%-90% confluency, BMSCs were trypsinized and passaged.

2.4 | Detection of labile iron pool (LIP)

The LIP can be quantified based on its ability of binding to cytomembrane permeable chelators, such as calcein acetoxymethyl ester (Calcein-AM). Calcein-AM undergoes hydrolysis by esterases to Calcein and gives out the green fluorescence after entering viable cells. LIP in the cells can combine with Calcein reversibly and then quench its fluorescence upon binding to cellular LIP, in a stochiometric fashion by detecting the mean fluorescent intensity (MFI) of Calcein. Cellular LIP was measured as following:

BMSCs were washed three times with DMEM culture solution without serum, then adjusted the density of different groups of BMSCs to 1×10^6/mL. Incubated 100 μL BMSCs mixed with 20 μL of Calcein-AM 0.125 μM (Sigma, St. Louis, MO, USA) protected from light for 5 min in the 5% CO_2 incubator at 37℃. At last, washed the cells with PBS by three times, and flow cytometry was finally used to detect the MFI of different treatments of BMSCs. The experiment was repeated three times, and results were presented as the mean values with standard deviations.

2.5 | Cell-Counting Kit-8 proliferation assay

BMSCs were seeded at 2000 cells/well in 96-well plates for 24 h, then the cell number was measured using Cell-Counting Kit-8 (CCK-8) proliferation assay kit (Beyotime

Biotechnology, China) according to the instruction. BMSCs were mixed with 100 μL culture medium and 10 μL of CCK-8 solution/well, and incubated for further 2 h at 37°C in a dark place. The amount of formazan dye generated by cellular dehydrogenase activity was measured for absorbance at 450 nm with a microplate reader. The optical density (OD) values of each well represented the survival/proliferation of BMSCs. The experiment was repeated three times, and results were presented as the mean values with standard deviations.

2.6 | EdU staining assay

The EdU staining assay was performed using the In Cell-Light EdU Apollo567 in Vitro Kit (Ribobio, Guangzhou, China) according to the manufacturer's instructions. Briefly, 10 μM EdU was added to BMSCs for 2 h. Cells were washed with PBS by three times, followed by 4% paraformaldchyde fixation. Then, BMSCs were incubated with 2 mg/mL glycine, and then washed with PBS by three times. After permeabilization with PBS containing 0.5% Triton X-100 and extensive washing with PBS twice, cells were incubated with staining solution for 30 min. Next, cells were washed with PBS containing 0.5% Triton X-100 for three times, followed by 15 min incubation with DAPI staining solution 20 μg/mL at room temperature. Images of the staining were captured with a fluorescent microscope (Olympus IX73). The experiment was repeated three times, and results were presented as the mean values with standard deviations.

2.7 | Senescence β-Galactosidase (β-gal) staining assay

β-gal activity was determined using a β-gal staining kit from Beyotime according to the manufacturer's instructions. BMSCs cultured in 6-well-plate were washed with PBS and fixed in 4% paraformaldehyde (m/v) for 15 min at room temperature. After rinsing with PBS,

cells were incubated with a freshly prepared β-gal staining solution for 16 h at 37°C. Under standard light microscopy (Nikon ECLIPSE TS100), the number of blue-staining cells, which identified to be the β-gal positive cells, was used to calculate the percentage of senescent cells with a total of 1000 cells in 10 randomly chosen fields. The experiment was repeated three times, and results were presented as the mean values with standard deviations.

2.8 | Reactive oxygen species (ROS) detection

ROS measurement was quantified by DCFH-DA fluorescence method as described previously and all procedures were protected from light. For ROS measurement, after being washed three times with PBS, BMSCs were loaded with DCFH-DA 10 μM to incubate for 30 min at 37°C. Cells were then washed with PBS by three times in order to fully remove the superfluous DCFH-DA probe which didn't penetrate into BMSCs. Next, BMSCs were fixed in 4% paraformaldehyde (m/v) for 30 min at room temperature. After being washed again with PBS by three times, the fixed cells were stained with DAPI 20 μg/mL for 15 min at room temperature. Then the cells were imaged with a fluorescent microscope (Olympus IX73). The experiment was repeated three times, and results were presented as the mean values with standard deviations.

2.9 | MitoSOX™ Red mitochondrial superoxide indicator (MitoSOX™ Red) assay

MitoSOX™ Red mitochondrial superoxide indicator was a novel fluorogenic dye for highly selective detection of superoxide in the mitochondria of live cells. MitoSOX™ Red reagent was live-cell permeant and was rapidly and selectively targeted to the mitochondria. Once in the mitochondria, MitoSOX™ Red reagent was oxidized by superoxide and exhibited red fluorescence. The MitoSOX™ Red assay was performed according to the manufacturer's

instructions. Briefly, dissolve the contents (50 μg) of one vial of MitoSOX™ Red mitochondrial superoxide indicator in 13 μL of DMSO to make a 5 mM MitoSOX™ reagent stock solution. Dilute the 5 mM MitoSOX™ reagent stock solution (prepared above) in HBSS/Ca/Mg to make a 5 μM MitoSOX™ reagent working solution. Apply 1 mL of 5 μM MitoSOX™ reagent working solution to cover cells adhering on 6-well-plate. Incubate cells for 10 min at 37°C protected from light. Wash cells gently by three times with warm buffer, and the stained cells with counterstains as desired and mounted in warm buffer for imaging with fluorescence microscope at 530/590 nm (Olympus IX73). The experiment was repeated three times, and results were presented as the mean values with standard deviations.

2.10 | Measurement of mitochondrial membrane potential (ΔΨm)

JC-1 Mitochondrial Membrane Potential Assay Kit (Abcam, UK) was used to measure the ΔΨm in BMSCs. JC-1 was a cationic dye that accumulated in energized mitochondrial. At a low concentration (due to low mitochondrial membrane potential), JC-1 was predominantly a monomer that yields green fluorescence with emission of 530 nm. At a high concentration (due to high mitochondrial membrane potential), the dye aggregated yields a red to orange colored emission of 590 nm. Therefore there is a significant decrease in the aggregate fluorescent count of indicative of depolarization whereas an increase is indicative of hyperpolarization. According to the manufacturer's instructions, 1×10^4 cells were seeded in a 24-well-plate and incubated with 1 × JC-1 in growth medium for 20 min at 37˚C and then rinsed twice with JC-1 washing buffer. Monomeric JC-1 green fluorescence mission and aggregate JC-1 red fluorescence emission were measured using a fluorescence microscope at 530/590 nm (Olympus IX73). The ΔΨm in each group was evaluated as the fluorescence

ratio of red to green. The experiment was repeated at least three times, and results were presented as the mean values with standard deviations.

2.11 | Osteogenic differentiation of BMSCs

For osteoblastic differentiation, when reaching 80%-90% confluence, the BMSCs were cultured in Mesenchymal Stem Cell Osteogenic Differentiation Medium (OS medium) (Cyagen Biosciences Inc, HUXMA-90021, China) supplemented with osteogenic inducers, including Mesenchymal Stem Cell Osteogenic Differentiation Basal Medium containing with 10% FBS, 100 U/mL penicillin-streptomycin, 1% glutamine, 10 nM dexamethasone, 0.2 mM L-ascorbic acid, and 10 mM β-glycerophosphate. The cells were cultured in differentiation medium for approximately 14 days with a medium change every 3 days. Then BMSCs were collected for qRT-PCR and western blot, or used to perform alizarin red S (ARS) staining and alkaline phosphatase (ALP) staining.

2.12 | Adipogenic differentiation of BMSCs

For adipogenic differentiation, when reaching 80%-90% confluence, the BMSCs were cultured in Mesenchymal Stem Cell Adipogenic Differentiation Medium (OA medium) supplemented with adipogenic inducers, including 175 mL Mesenchymal Stem Cell Adipogenic Differentiation Basal Medium A supplemented with 20 mL Mesenchymal Stem Cell-Qualified Fetal Bovine Serum, 2 mL penicillin-streptomycin, 2 mL glutamine, 200 μL dexamethason, 200 μL rosiglitazone, 400 μL insulin and 200 μL 3-isobutyl-1-methyl-xanthine, as well as 175 mL Mesenchymal Stem Cell Adipogenic Differentiation Basal Medium B supplemented with 20 mL Mesenchymal Stem Cell-Qualified Fetal Bovine Serum, 2 mL penicillin-streptomycin, 2 mL glutamine and 400

μL insulin. BMSCs were seeded at density of 5×10^5 cells per well in a 12-well-plate. The OA medium was replaced every 3 days. On the 14th day of adipogenic differentiation, BMSCs were collected for qRT-PCR and western blot, or used to perform oil red O staining.

2.13 | Alizarin red S (ARS) staining

On the 14th day of osteogenic differentiation, OS medium was discarded and ARS staining was performed to detect matrix mineralization deposition. Briefly, BMSCs were gently washed with PBS solution by three times, the cells were fixed with 4% paraformaldehyde (m/v) for 10 min at room temperature. Then cells were washed with PBS solution by three times and stained with 40 mM alizarin red S (pH 4.2) for 15 min at 37°C. Then after washing three times with PBS solution, the stained cells in each well were photographed under a standard light microscopy (Nikon ECLIPSE TS100). The orange and red positions were recognized as calcium deposits. The ARS staining was repeated three times independently. Ten photos were taken randomly for each well. The ARS staining was quantified using Image Pro Plus 6.0 (Media Cybernetics, USA).

2.14 | Alkaline phosphatase (ALP) staining

On the 14th day of osteogenic differentiation, OS medium was discarded and ALP staining was performed to detect matrix mineralization deposition. Briefly, cells in 12-well-plate were gently washed with PBS solution by three times, then the cells were fixed with 95% ethanol for 10 min at room temperature. After washing with PBS solution by three times, cells were stained with the ALP neutral buffer staining solution (pH 9.4), including 3% β-glycerophosphate disodium salt hydrate, 2% sodium pentobarbital, 2% calcium chloride, 2% magnesium sulfate and ddH_2O, for 4 h at 37°C. Next, 2% cobalt nitrate was added in

each well and incubated for 5 min at room temperature. After washing with PBS solution by three times, 1% ammonium sulfide was added in each well and incubated for 2 min at room temperature. After washing three times with PBS solution, the stained cells in each well were photographed under a standard light microscopy (Nikon ECLIPSE TS100). The black and grey, insoluble, granular dye deposits indicated the activity of alkaline phosphatase, which were recognized as matrix mineralization deposition. The ALP staining was repeated by three times independently with 10 photos were taken randomly for each well each time. The staining was quantified using Image Pro Plus 6.0 (Media Cybernetics, USA).

2.15 | Oil red O Staining

On the 14th day of adipogenic differentiation, OA medium was discarded and oil red O staining was accomplished according to the procedures provided by the manufacturers. Briefly, cells in 24-well-plate were gently washed with PBS solution by three times, then the cells were fixed with 4% paraformaldehyde (m/v) for 30 min at room temperature. After washing three times with PBS solution, cells were then incubated with oil red O working solution (oil red O stocking solution: ddH_2O = 3: 2; oil red O stocking solution was 0.5% oil red O in isopropanol) for 20 min at room temperature. Then the working solution was removed, and cells were washed three times with PBS solution. The stained cells in each well were photographed under a standard light microscopy (Nikon ECLIPSE TS100) and the oil red O staining was repeated for three times independently with ten photos were taken randomly for each well each time. The staining was quantified using Image Pro Plus 6.0 (Media Cybernetics, USA).

2.16 | Animal experiments

Iron dextran solution was injected by intraperitoneal injection to establish a mouse model of iron overload. A total of 30 C57BL/6J mice were randomly divided into three groups (n = 10/group)：sham group, iron overload group and iron overload with melatonin group. Mice from sham group were injected with 300 μL normal saline by intraperitoneal injection everyday for two weeks. Mice from iron overload group were injected with 300 μL iron dextran (diluted by normal saline to 100 mg/mL) everyday for two weeks. And the mice from iron overload with melatonin group were received intraperitoneal injection with the same dose of iron dextran as the iron overload group, as well as with melatonin 10 μg/g everyday for two weeks. All mice were sacrificed after 14 days treatment and the BMSCs from different groups were collected. Iron overload was confirmed by LIP. ARS staining and ALP staining were applied to analyze the osteogenic differentiation potential of BMSCs from iron dextran-treated mice. Oil red O staining was applied to test the adipogenic differentiation potential of BMSCs from iron dextran-treated mice. The stained cells were photographed under a standard light microscopy.

2.17 | Total RNA extraction and quantitative reverse transcription-polymerase chain reaction (qRT-PCR)

Total RNA from different groups of BMSCs per experimental condition was extracted with TRIzol reagent (Invitrogen, CA, USA) according to the manufacturer's instructions, cDNA was prepared using the High-Capacity cDNA Reverse Transcription Kits (Applied Biosystems, Foster City, CA, USA) following the manufacturer's protocol. qRT-PCR was performed on ABI 7500 real-time PCR system (Applied Biosystems, Foster City, CA, USA).

Conditions were as follows: hold stage was 95°C for 10 min, cycling was 40 cycles of 95°C for 30 s, 60°C for 30 s, and 72°C for 30 s. Expression of the following genes was examined: alkaline phosphatase (ALP), Collagen type I (Collagen-I), bone morphogenetic protein 2 (BMP2), bone morphogenetic protein 4 (BMP4), runt-related transcription factor 2 (Runx2), Osterix, Spp1 (osteopontin), BGLAP (osteocalcin), peroxisome proliferator activated receptor γ (PPARγ) and (CCAAT-enhancer-binding protein α) C/EBPα. The level of expression of glyceraldehyde-3-phosphate dehydrogenase (GAPDH) gene served as reference. The forward and reverse primer sequences used in our experiments were listed in TABLE 1. Each qRT-PCR was processed in triplicate. The threshold cycle (Ct) value was subsequently determined, and the relative quantification of mRNA expression was calculated using the comparative Ct method.

2.18 | Western blot

The protocol for western blot was based on previous reports. Briefly, BMSCs were lysed in ice-cold cell lysis buffer (Beyotime), containing protease inhibitors, and the protein concentration in cell extracts was quantified using a BCA protein assay kit (Beyotime) following the manufacturer's recommended protocol. Equal amounts (50 μg) of protein from each extract were denatured and resolved using a 12.5% SDS-PAGE, and then transferred by electrophoresis onto a nitrocellulose membrane (Millipore, Billerica, MA). Nonspecific proteins were blocked by incubating nitrocellulose membranes in blocking buffer (5% non-fat dry milk in T-TBS containing 0.05% Tween-20) for 1 h at room temperature and then the nitrocellulose membranes were incubated overnight at 4℃with primary antibodies against: phospho-ERK (1: 1000, Cell Signaling Technology), total-ERK (1:1000, Cell Signaling

Technology), phospho-p38 (1:1000, Cell Signaling Technology), total-p38 (1:1000, Cell Signaling Technology), total-p53 (1:1000, Cell Signaling Technology), p16 (1:1000, Abcam), p21 (1:1000, Abcam) and GAPDH (1:1000, Abcam). After rinsing, the nitrocellulose membranes were incubated in horseradish peroxidase-conjugated secondary antibodies (1:2000, Cell Signaling Technology) as a secondary antibody for 1 h incubation at room temperature. The washing procedure was repeated six times within one hour. Immunoreactive bands were visualized by the Odyssey Infrared Imaging System. For purposes of quantification, the intensity of each band was quantified using the ImageJ Software (National Institutes of Health, Bethesda, MD, USA). The GAPDH protein was used as an internal loading control.

2.19 | Statistical analysis

All experiments were performed with BMSCs from three to ten independent groups, number of samples (*n*) for each experiment was indicated in the corresponding figure legend. Quantitative data were presented as mean ± SEM. Statistical analysis was performed using oneway ANOVA followed by Newman-Keules or Student's t-test with the SPSS 16.0 statistical software (SPSS, Chicago, IL, USA). A probability value $p < 0.05$ (*), $p < 0.01$ (**) or $p < 0.001$ (***) was considered to be statistically significant.

3 | RESULTS

3.1 | FAC-induced iron overload caused the decrease of cell viability in BMSCs

Initially, to determine if iron overload could induce the injury on BMSCs, we treated BMSCs with FAC 50 μM, 100 μM, 200 μM and 400 μM for 24 h. Morphological observation

demonstrated that the cells exposed to FAC treatment showed irregularly morphological changes. More shrinkage cells and visible floating cells were observed in FAC treatment groups, and the cell density decreased with different concentrations of FAC in a dose-dependent manner. Especially, treatment with FAC 400 μM resulted in the vast majority of cell floating and death of BMSCs (Figure 1A). Labile iron pool (LIP) assay showed that exposure to FAC 50 μM, 100 μM, 200 μM and 400 μM caused concentration-dependent iron overload in BMSCs (Figure 1B). Meanwhile, with the concentration of FAC increasing from 50 μM to 400 μM, the viability of BMSCs was gradually decreased (Figure 1C). A majority of BMSCs was observed dead after treated with FAC 400 μM but not 200 μM. Whereas, a sublethal concentration of FAC at 200 μM lead to the injury of BMSCs without the majority of BMSCs dead. Therefore, FAC 200 μM was used as the optimal dosage in the further investigation.

3.2 | Melatonin protected BMSCs against FAC-induced inhibition of osteogenic differentiation

First, we analyzed whether osteogenic potential of BMSCs was affected by FAC-induced iron overload and rescued by melatonin supplementation. The osteogenic differentiation of BMSCs were successfully induced by 14-day culture in OS medium, as shown by the positive staining for ARS staining (Figure 2A) and ALP staining (Figure 2B). We found that FAC-induced iron overload markedly inhibited differentiation of BMSCs into osteoblast lineage. However, melatonin-treated BMSCs showed a concentration dependent increase in mineralized areas from 10 nM to 100 μM. To further evaluate the propensity for osteogenic differentiation, the transcription levels of osteoblast-specific genes including ALP, Collagen-I,

BMP2 and BMP4 were examined. Exposure to FAC 200 μM significantly reduced the expression of osteoblast-specific genes compared to control group. In contrast, melatonin treatment reversed the downregulation of osteoblast-specific genes at mRNA level in FAC-treated BMSCs (Figure 2C). The osteogenic transcription factors Runx2, Osterix, Spp1 and BGLAP were required for the commitment of BMSCs into osteoblast lineage. qRT-PCR assay showed that these osteogenic transcription factors decreased after exposure to FAC 200 μM, but treatment with melatonin 10 nM, 1 μM and 100 μM increased the mRNA levels (Figure 2D). These results suggest that melatonin restores the osteogenic differentiation potential of FAC-treated BMSCs.

3.3 | Melatonin prevented adipogenic differentiation of BMSCs in response to FAC

Furthermore, oil red O staining was applied to evaluate the effects of iron overload and melatonin on adipogenic potential of BMSCs after cultured in OA-medium for 14-day. Oil red O staining showed that FAC-induced iron overload promoted the differentiation of BMSCs into adipogenic lineage. But, melatonin-treated BMSCs showed a decrease quantity of red oil drops ranging from melatonin 10 nM to 100 μM (Figure 3A). Meanwhile, the expressions of adipogenic-specific genes including PPARγ and C/EBPα were examined as well. Exposure to FAC 200 μM increased the expression of adipogenic-specific genes PPARγ and C/EBPα compared to control group, which was partially reversed by melatonin 10 nM, 1 μM and 100 μM (Figure 3B). These results suggest that melatonin inhibits the adipogenic differentiation of FAC-treated BMSCs.

3.4 | Effects of melatonin on FAC-induced proliferation reduction and senesence of BMSCs

Next, we investigated whether FAC induced the senescence of BMSCs and if melatonin could protect BMSCs against aging. β-gal staining was performed to observe the appearance of senescent BMSCs. As shown in Figure 4A and 4B, a significant increase of β-gal-positive cells was observed in the FAC-treated BMSCs. Only 2.93% cells were positive for β-gal staining in control group, but the percentage of β-gal-positive cells was increased to 70.56% after treating with FAC 200 μM. Treatment with melatonin at 10 nM, 1 μM and 100 μM could significantly decrease the percentage of β-gal-positive senescent BMSCs to 58.33%, 45.60% and 42.42% respectively. This result suggests that melatonin is capable of effectively suppressing the senescence of BMSCs induced by iron overload. Cellular senescence usually accompanies with the reduction of proliferation. We then investigated if FAC-induced iron overload inhibited the growth of BMSCs, and whether melatonin produced protective and pro-proliferative effects on BMSCs. Firstly, exposed to FAC 200 μM resulted in a significant morphological destruction in BMSCs compared to control group, while this alteration was remarkably attenuated in the presence of different concentrations of melatonin treatment (Figure 4C). CCK-8 assay confirmed that cell viability was significantly inhibited by FAC 200 μM treatment, while melatonin treatment induced a gradual increase of viability of BMSCs at concentrations ranging from 10 nM to 100 μM (Figure 4D). Afterwards, we examined the pro-proliferative effect of melatonin on BMSCs by EdU staining. As shown in Figure 4E and 4F, the BMSCs exhibited less EdU-positive staining compared to control group when treated with FAC 200 μM for 24 h. However, in the presence of different

concentrations of melatonin, BMSCs showed a concentration dependent increase of EdU-positive staining compared to the FAC group. These results indicate that melatonin plays a pro-proliferative role in iron overload-induced proliferation inhibition of BMSCs.

3.5 | Effect of melatonin inhibitor luzindole on FAC-induced osteogenic differentiation of BMSCs

Luzindole, a nonselective antagonist of melatonin receptor, was used to determine whether the effects of melatonin on FAC-induced BMSCs were mediated through the melatonin receptor pathway. We further studied if luzindole is involved in the protective effect of melatonin on osteogenic and adipogenic of BMSCs. ARS staining (Figure 5A) and ALP staining (Figure 5B) showed that luzindole treatment blocked melatonin induced increase of mineralized areas in FAC-treated BMSCs. qRT-PCR also showed that the augment expression of osteoblast-specific genes including ALP, Collagen-I, BMP2 and BMP4 in FAC-treated BMSCs by melatonin was partially reversed by luzindole 10 μM treatment (Figure 5C). Meanwhile, luzindole 10 μM decreased the transcription factors Runx2, Osterix, Spp1 and BGLAP mRNA levels (Figure 5D). These results indicate that luzindole inhibited the differentiation of BMSCs into the osteoblast lineage by blocking melatonin receptor.

3.6 | Effect of melatonin inhibitor luzindole on FAC-induced adipogenic differentiation of BMSCs

Next, oil red O staining showed that melatonin-induced the decrease of red oil drops in FAC-induced BMSCs was also reversed by luzindole 10 μM supplementation (Figure 6A). Meanwhile, luzindole also abolished melatonin-induced downregulation of adipogenic-specific genes PPARγ and C/EBP-α in FAC-treated BMSCs (Figure 6B). These

results suggest that luzindole could promote the differentiation of BMSCs into the adipogenic lineage by blocking melatonin receptor.

3.7 | Melatonin inhibitor luzindole abolished FAC-induced proliferation reduction and senesence of BMSCs

β-gal staining showed that melatonin 100 μM inhibited the β-gal-positive senescent BMSCs compared to the FAC 200 μM group, which could be also reversed by luzindole 10 μM (Figure 7A and 7B). This result suggests that luzindole effectively inhibited the suppressing of senescence induced by melatonin on FAC-treated BMSCs. In addition, melatonin 100 μM significantly attenuated FAC-induced the decrease of viability of BMSCs, but this improvement could be markedly blocked by luzindole 10 μM (Figure 7C). Similarly, we also confirmed the role of luzindole on the proliferation of BMSCs by EdU staining. As shown in Figure 7D and 7E, melatonin 100 μM could improve the proliferation of FAC-treated BMSCs, but in the presence of luzindole 10 μM, melatonin failed to ameliorate FAC-induced proliferation reduction of BMSCs. These results indicate that melatonin play a protective role in FAC-induced BMSCs dysfunction through melatonin receptor. Taken together, these results suggest that the protective effect of melatonin on iron overload-induced BMSCs dysfunction is mediated by activation of melatonin membrane receptor.

3.8 | Melatonin prevented iron dextran-induced inhibition of osteogenic differentiation and promotion of adipogenic differentiation in vivo

An iron overload mouse model was established by intraperitoneally injecting with iron dextran and melatonin everyday for 14 days to observe the iron overload injury in BMSCs and the protective effects of melatonin. To confirm the establishment of iron overload mouse

model, BMSCs were collected after 2 weeks treatment and LIP of BMSCs were dynamically detected. LIP showed that the treatment of iron dextran caused a significant iron overload in BMSCs compared to the sham group by decreasing the MFI, while melatonin treatment could improve the MFI in iron dextran-treated BMSCs (Figure 8A). ARS staining and ALP staining showed that iron dextran-induced iron overload markedly inhibited differentiation of BMSCs into osteoblast lineage. However, with the treatment of melatonin in BMSCs showed a increase in mineralized areas (Figure 8B-8C). Besides, oil red O staining showed that melatonin treatment decreased the red oil drops compared to iron dextran-treated BMSCs (Figure 8D). These results validate that the iron overload injury induced by iron dextran in BMSCs and the osteogenic differentiation protective effect of melatonin in iron overload-induced BMSCs in vivo.

3.9 | Melatonin reversed FAC-induced increase of ROS in BMSCs

It is well documented that ROS are involved in iron overload-induced cell injury and organ aging. Oxidant stress has been shown to initiate and promote apoptosis and senescence via oxidizing mitochondrial membrane phospholipids and depolarizing mitochondrial membrane potential.[32] To reveal the mechanism of melatonin antagonizing FAC-induced BMSCs dysfunction, effects of melatonin on the production of ROS was investigated by DCFH-DA probe. As shown in Figure 9, intracellular ROS level was increased in the presence of FAC 200 μM for 24 h, which was reversed by treatment with melatonin 100 μM. This result suggest that ROS-mediated oxidant stress was involved in iron overload-induced BMSCs.

3.10 | Melatonin reversed FAC-induced mitochondrial dysfunction in BMSCs

Then, we further studied if the increase of intracellular ROS level occuring in the mitochondria. The superoxide production in the mitochondria was measured using MitoSOX™ Red mitochondrial superoxide indicator assay. Treatment of BMSCs with FAC 200 μM for 24 h led to an increase of mitochondrial superoxide productions manifested by the increasing red fluorescence, while the red fluorescence could be inhibited by treatment with melatonin 100 μM (Figure 10A). In addition, we further investigated whether mitochondrial dysfunction is involved in protection of melatonin against FAC-induced BMSCs dysfunction. The disruption of mitochondrial membrane potential was observed by JC-1 staining. As shown in Figure 10B, treatment of BMSCs with FAC 200 μM for 24 h caused the loss of mitochondrial membrane potential, which could be ameliorated by treatment with melatonin 100 μM. These results indicate that ROS-mediated mitochondrial dysfunction was involved in iron overload-induced dysfunction of BMSCs.

3.11 | Melatonin suppressed FAC-induced BMSCs injury by blocking p53/ERK/p38 signal pathway

Recently, it was reported that p53, ERK and p38 signal pathway could activate the downstream genes of ROS and led to cellular senescence, apoptosis and the inhibition of differentiation. Therefore, we assessed if the protein expressions of p53, ERK and p38 signal pathway changed in FAC-induced process. In our study, we examined the protein expression levels of p53, p21, p16, phosphorylated and total protein levels of ERK and p38 in each group using western blot analysis. The relative expression was normalized to GAPDH and illustrated in Figure 11. As expected, treatment of BMSCs with FAC 200 μM for 24 h caused

the increasing protein expressions of p53, p21 and p16, phosphorylated and total ERK and p38 compared to the control group. While, in the presence of melatonin 100 μM, melatonin ameliorated the increased the protein expressions of p53, p21 and p16, as well as phosphorylated and total ERK and p38 in FAC-treated BMSCs. These results indicated that FAC-induced injury of BMSCs was associated with ROS accumulation as well as p53/ERK/p38 signal pathway activation. The ROS-mediated mitochondrial dysfunction was involved in iron overload–induced dysfunction of BMSCs.

4 | DISCUSSION

In the present study, we firstly revealed that iron overload induced by FAC inhibited the proliferation and osteogenic differentiation, promoted the senescence by increasing mitochondrial ROS accumulation and depolarizing mitochondrial membrane potential of BMSCs, which was effectively rescued by melatonin. These findings help us towards a better understanding of the mechanisms underlying melatonin treating FAC-induced BMSCs dysfunction and related bone diseases.

4.1 | Iron overload as a new risk factor for BMSCs dysfunction

BMSCs have the ability for self-renewal and multiple differentiation potentials.[32] Numerous studies have shown that BMSCs can differentiate into osteoblasts, chondrocytes and adipocytes. Therefore BMSCs seem to be the one of greatest therapeutic resources for gene therapy, cell therapy and tissue engineering.[33] Especially, BMSCs have been proved to be an important role in maintaining bone mass and balancing bone marrow microenvironment.[33] Iron overload is a disorder of iron metabolism. It could be induced by hereditary

hemochromatosis or multiple blood transfusions for diseases such as beta thalassemia and bone marrow failure.[34,35] Recently, more and more evidence show that excess iron can lead to toxic effects on the proliferation and differentiation of BMSCs, and iron overload is correlated with bone mass loss and osteoporosis.[35,36] However, how to prevent iron overload induced injury in BMSCs has not been fully affirmed yet.

4.2 | Potential of melatonin as a protective drug for iron overload-induced BMSCs dysfunction

Melatonin is a key endogenous indole amine secreted and released by pineal gland of mammals, it mainly involves in the regulation of circadian rhythms, seasonal reproduction, cardiovascular function and immune function.[37] Many studies have demonstrated that melatonin played a critical role in scavenging free radicals, stimulating antioxidant enzymes and anti-inflammatory. In our study, we hypothesized that melatonin played a protective role in iron overload-induced BMSCs dysfunctions.

First of all, the osteogenic and adipogenic potential of BMSCs in vitro were tested. qRT-PCR showed that the expressions of osteoblast-specific genes (collagen-I, ALP, BMP2, and BMP4) and osteogenesis related transcription factors (Runx2, Osterix, Spp1 and BGLAP) were significantly decreased by FAC treatment, while remarkably increased by different concentrations of melatonin supplementation. On the contrary, adipogenic-specific genes, including PPARγ and C/EBPα were increased by FAC treatment, while decreased by different concentrations of melatonin treatment. Moreover, ARS staining and ALP staining for osteogenesis identification, oil red O staining for adipogenesis identification confirmed the protective function of melatonin in FAC-induced BMSCs. These results suggest that

melatonin has a protective effect of osteogenic differentiation in FAC-induced BMSCs.

In order to demonstrate whether FAC could lead to senescence of BMSCs, we further used β-gal staining to assess BMSCs senescence, and result showed that BMSCs underwent senescence in the presence of FAC 200 μM, which could be reversed by melatonin 10 nM, 1 μM and 100 μM. This data suggest that melatonin exerts anti-senescent effect after FAC-induced iron overload of BMSCs. Consistently, morphological observation, CCK8 assay and EdU staining showed that BMSCs treated with FAC 200 μM combined with melatonin 10 nM, 1 μM and 100 μM could significantly increased the cellular viability and promoted the proliferation.

4.3 | The underlying mechanism of melatonin preventing against iron overload-induced BMSCs toxicity

A large number of studies have demonstrated that iron overload led to an increase in cellular ROS and negatively affected vital organs, such as the liver, heart, brain and bones.[38] The over accumulation of ROS and oxidative stress play a key role in the development of cellular senescence and death. It has been shown that iron overload induced the death of BMSCs via increasing intracellular ROS level.[38] Meanwhile, numerous reports have demonstrated that melatonin is a particularly effective endogenous antioxidant which acts not only as a direct scavenger of free radicals but also induces the enzymes that metabolize free radicals.[38] Thus, we explored whether melatonin protects BMSCs against iron overload-induced BMSCs injury via influencing ROS level. The ROS fluorescent probe was further used to detect the level of intracellular ROS in BMSCs. We found that ROS in BMSCs treated by FAC 200 μM was markedly increased, while treatment with melatonin can reverse this process, indicating

FAC-induced ROS accumulation is involved in BMSCs dysfunction. As a type of antioxidant, melatonin could maintain the mitochondrial homeostasis, and it has been found to be protective against mitochondrial oxidative damage under various pathological conditions, including hypoxia, ischemia, high fat, and metabolic poisons-induced toxic reaction. Mitochondria is believed to be the major source of ROS production, therefore mitochondrial ROS and mitochondrial membrane potential were studied in FAC-treated BMSCs by using MitoSOX^{TM} Red staining and JC-1 assay. We found that melatonin treatment can attenuate the increase of ROS production by FAC treatment and rescue the loss of mitochondrial membrane potential by melatonin treatment. These data suggest that melatonin protects against FAC-induced BMSCs dysfunction via inhibiting ROS accumulation.

5 | CONCLUSION

In summary, the data of our current study suggested that melatonin have the capacity of rescuing iron overload-induced inhibition of proliferation and osteogenic differentiation in BMSCs, and at the same time reverse the senescence in iron overload-induced BMSCs by blocking ROS accumulation as well as p53/ERK/p38 activation. These findings help us towards a better understanding of the mechanisms underlying melatonin treating FAC-induced BMSCs dysfunction and related bone diseases.

ACKNOWLEDGEMENTS

We thank Simon Chen from University of Calgary for his valuable technical support regarding data quantification.

FUNDING INFORMATION

This study was supported by the Natural Science Foundation of China (81501920/81573434), the Natural Science Foundation of Heilongjiang Province (LC2015027/ H2015056), the Fundation for Creative Research Groups (81421063), and Special Research Fundation for Doctoral Courses (20132307120023).

DISCLOSURES

The authors had no conflicts of interest to declare in relation to this article.

AUTHORS' CONTRIBUTION

Benzhi Cai and Lei Yang: conception and design, provision of study materials, manuscript writing; Fan Yang, Yuan Li, Gege Yan, Chao Feng, Tianyi Liu, Rui Gong, Ye Yuan, Elina Idiiatullina, Timur Bikkuzin, Valentin Pavlov, Yang Li, Chaorun Dong, Dawei Wang, Yang Cao, Zhenbo Han, Lai Zhang, Qi Huang and Fengzhi Ding: collection and assembly of data; Fan Yang, Yuan Li and Ye Yuan: data analysis and interpretation; Benzhi Cai, Ning Wang, Lei Yang and Zhengang Bi: financial support, final approval of manuscript.

FIGURE LEGEND

FIGURE 1 FAC-induced iron overload caused the decrease of cell viability in BMSCs. (A) BMSCs exposed to FAC showed fibroblastic morphological changes and reduced cell density compared to the cells without FAC treatment. Moreover, treatment with FAC 400 μM resulted in cell floating and death on most of BMSCs; (B) Labile iron pool (LIP) assay

showed that exposure to FAC 50 μM, 100 μM, 200 μM and 400 μM caused concentration-dependent iron overload in BMSCs; (C) CCK-8 assay showed that Mel played a significant protective role in the cellular viability of BMSCs in a dose-dependent manner for 24 h. Values are the mean ± SEM of 3 independent experiments (n = 3). * $p < 0.05$, ** $p < 0.01$, *** $p < 0.001$.

FIGURE 2 Melatonin protected BMSCs against FAC-induced inhibition of osteogenic differentiation. (A-B) ARS and ALP staining were used to evaluate the osteogenic differentiation ability of different concentrations of melatonin in FAC-induced BMSCs. Results showed that FAC-induced iron overload markedly inhibited the differentiation of BMSCs into osteoblast lineage. However, melatonin-treated BMSCs showed a concentration-dependent increase of mineralized areas from 10 nM to 100 μM melatonin treatment; (C-D) The transcription levels of osteoblast-specific genes (ALP, Collagen-I, BMP2 and BMP4) and osteogenic transcription factors (Runx2, Osterix, Spp1 and BGLAP) were examined by qRT-PCR to evaluate the osteogenic differentiation ability of melatonin in FAC-induced BMSCs. qRT-PCR assay showed that these factors involved in the osteogenic differentiation decreased after exposure to FAC 200 μM, but treatment with melatonin 10 nM, 1 μM and 100 μM increased the mRNA levels. Values are the mean ± SEM of 3 independent experiments (n = 3). * $p < 0.05$, ** $p < 0.01$, *** $p < 0.001$.

FIGURE 3 Melatonin prevented adipogenic differentiation of BMSCs in response to FAC. (A) Oil red O staining results showed that FAC-induced iron overload promoted the differentiation of BMSCs into adipogenic lineage. But, melatonin-treated BMSCs showed a decrease quantity of red oil drops ranging from melatonin 10 nM to 100 μM; (B)

Transcription levels of adipogenic-specific genes including PPARγ and C/EBPα were examined by qRT-PCR. Results showed that exposure to FAC 200 μM increased the expression of adipogenic-specific genes PPARγ and C/EBPα compared to control group, which was partially reversed by melatonin 10 nM, 1 μM and 100 μM. Values are the mean ± SEM of 3 independent experiments ($n = 3$). ** $p < 0.01$, *** $p < 0.001$.

FIGURE 4 Effects of melatonin on FAC-induced proliferation reduction and senesence of BMSCs. (A-B) β-gal staining showed that a significant increase of β-gal-positive cells was observed in the FAC-treated BMSCs, while treatment with melatonin at 10 nM, 1 μM and 100 μM could significantly decrease the percentage of β-gal-positive senescent BMSCs to varying degrees respectively; (C) Morphological observation revealed that exposed to FAC 200 μM resulted in a significant morphological destruction in BMSCs compared to control group, while this alteration was remarkably attenuated in the presence of different concentrations of melatonin treatment; (D) CCK-8 assay result confirmed that cell viability was significantly inhibited by FAC 200 μM treatment, while melatonin treatment induced a gradual increase of viability of BMSCs at concentrations ranging from 10 nM to 100 μM; (E-F) EdU assay results proved that BMSCs exhibited less EdU-positive staining compared to control group when treated with FAC 200 μM for 24 h. However, in the presence of different concentrations of melatonin, BMSCs showed a concentration-dependent increase of EdU-positive staining compared to the FAC group. Values are the mean ± SEM of 3 independent experiments ($n = 3$). * $p < 0.05$, *** $p < 0.001$.

FIGURE 5 Effect of melatonin inhibitor luzindole on FAC-induced osteogenic differentiation of BMSCs. (A-B) ARS staining and ALP staining showed that luzindole

treatment blocked melatonin-induced the increase of mineralized areas in FAC-treated BMSCs; (C-D) The transcription levels of osteoblast-specific genes (ALP, Collagen-I, BMP2 and BMP4) and osteogenic transcription factors (Runx2, Osterix, Spp1 and BGLAP) were examined by qRT-PCR to evaluate the osteogenic differentiation ability of luzindole and melatonin in FAC-induced BMSCs. qRT-PCR results showed that luzindole abolished melatonin-induced upregulation of osteoblast-specific genes and osteogenic transcription factors in FAC-treated BMSCs. Values are the mean ± SEM of 3 independent experiments (n = 3). * $p < 0.05$, ** $p < 0.01$, *** $p < 0.001$.

FIGURE 6 Effect of melatonin inhibitor luzindole on FAC-induced adipogenic differentiation of BMSCs. (A) Oil red O staining showed that melatonin-induced the decrease of red oil drops in FAC-induced BMSCs was reversed by luzindole 10 μM supplementation; (B) qRT-PCR results showed that luzindole abolished melatonin-induced downregulation of adipogenic-specific genes PPARγ and C/EBPα in FAC-treated BMSCs. Values are the mean ± SEM of 3 independent experiments (n = 3). ** $p < 0.01$, *** $p < 0.001$.

FIGURE 7 Melatonin inhibitor luzindole abolished FAC-induced proliferation reduction and senesence of BMSCs. (A-B) β-gal staining showed that melatonin 100 μM inhibited the β-gal-positive senescent BMSCs compared to the FAC 200 μM group, which could be also reversed by luzindole 10 μM; (C) CCK-8 result showed that melatonin 100 μM significantly attenuated FAC-induced the decrease of viability of BMSCs, but this improvement could be markedly blocked by melatonin inhibitor luzindole 10 μM; (D-E) EdU assay result showed that melatonin 100 μM could improve the proliferation of FAC-treated BMSCs, but in the presence of luzindole 10 μM, melatonin fail to ameliorate FAC-induced proliferation

reduction of BMSCs. Values are the mean ± SEM of 3 independent experiments (n = 3). * p < 0.05, ** p < 0.01, *** p < 0.001.

FIGURE 8 Melatonin prevented iron dextran-induced inhibition of osteogenic differentiation and promotion of adipogenic differentiation in vivo. (A) LIP was tested by flow cytometry to confirm the establishment of iron overload mouse model; (B-C) ARS staining and ALP staining were used to evaluate the osteogenic differentiation ability of melatonin in iron dextran-induced iron overload of BMSCs. Stainings showed that iron dextran-induced iron overload markedly inhibited differentiation of BMSCs into osteoblast lineage. However, melatonin-treated BMSCs showed an increase of mineralized areas; (D) Oil red O staining results showed that iron dextran-induced iron overload promoted the differentiation of BMSCs into adipogenic lineage. But, melatonin cotreatment on BMSCs showed a decrease quantity of red oil drops. Values are the mean ± SEM of 3 independent experiments (n = 3). *** p < 0.001.

FIGURE 9 Melatonin reversed FAC-induced increase of ROS in BMSCs. DCFH-DA probe was applied to evaluate the effect of luzindole and melatonin on the production of intracelluar ROS in FAC-induced BMSCs. Results showed that intracellular ROS level was increased in the presence of FAC 200 μM for 24 h, which was reversed by treatment with melatonin 100 μM. Values are the mean ± SEM of 3 independent experiments (n = 3). ** p < 0.01.

FIGURE 10 Melatonin reversed FAC-induced mitochondrial dysfunction in BMSCs. (A) Superoxide production in the mitochondria was measured using MitoSOX™ Red assay. Treatment of BMSCs with FAC 200 μM for 24 h led to an increase of mitochondrial superoxide productions manifested by the increasing red fluorescence, while the red

fluorescence could be inhibited by treatment with melatonin 100 μM; (B) The JC-1 probe detection result showed that treatment of BMSCs with FAC 200 μM for 24 h caused the loss of mitochondrial membrane potential, which could be ameliorated by treatment with melatonin 100 μM. Values are the mean ± SEM of 3 independent experiments (n = 3). *** p < 0.001.

FIGURE 11 Melatonin suppressed FAC-induced BMSCs injury by blocking p53/ERK/p38 signal pathway. Western blot results showed that the protein expression levels of p53, p21, p16, phosphorylated and total protein levels of ERK and p38 significantly increased in FAC-treatment groups compared to the control group. While, in the presence of melatonin 100 μM, melatonin ameliorated the increased the protein expressions of p53, p21 and p16, as well as phosphorylated and total ERK and p38 in FAC-treated BMSCs. Values are the mean ± SEM of 3 independent experiments (n = 3).

TABLE 1 The forward and reverse primers used for qRT-PCR

Target genes		**primer sequences**
ALP	Forward	5'-ACAACCTGACTGACCCTTCG-3'
	Reverse	5'-TCATGATGTCCGTGGTCAAT-3'
Collagen-I	Forward	5'-CAGCCGCTTCACCTACAGC-3
	Reverse	5'-TTTTGTATTCAATCACTGTCTTGCC-3'
BMP2	Forward	5'-CCTTGCTGACCACCTGAACT-3'
	Reverse	5'-AACATGGAGATTGCGCTGA-3'

BMP4	Forward	5'-TCGTTACCTCAAGGGAGTGG-3'
	Reverse	5'-ATGCTTGGGACTACGTTTGG-3'
Runx2	Forward	5'-AGAAGGCACAGACAGAAGCTTGA-3'
	Reverse	5'-AGGAATGCGCCCTAAATCACT-3'
Osterix	Forward	5'-AGAGGTTCACTCGCTCTGACGA-3'
	Reverse	5'-TTGCTCAAGTGGTCGCTTCTG-3'
Spp1	Forward	5'-ACACTTTCACTCCAATCGTCC-3'
	Reverse	5'-TGCCCTTTCCGTTGTTGTCC-3'
BGLAP	Forward	5'-TTCTGCTCACTCTGCTGACC-3'
	Reverse	5'-TTTGTAGGCGGTCTTCAAGC-3'
PPARγ	Forward	5'-TCACAAGAGGTGACCCAATG-3'
	Reverse	5'-CCATCCTTCACAAGCATGAA-3'
C/EBPα	Forward	5'-GTGTGCACGTCTATGCTAAACCA-3'
	Reverse	5'-GCCGTTAGTGAAGAGTCTCAGTTTG-3'
GAPDH	Forward	5'-CATCACTGCCACCCAGAAGAC-3'
	Reverse	5'-CCAGTGAGCTTCCCGTTCAG-3'

Abbreviations: ALP, alkaline phosphatase; Collagen-I, Collagen type I; BMP2, bone morphogenetic protein 2; BMP4, bone morphogenetic protein 4; Runx2, runt-related transcription factor 2; Spp1, osteopontin; BGLAP, osteocalcin; PPARγ, peroxisome proliferator activated receptor γ; C/EBPα, CCAAT-enhancer-binding protein α.

REFERENCES

1. BIANCO P, ROBEY PG , SIMMONS PJ. Mesenchymal stem cells: revisiting history, concepts, and assays. *Cell Stem Cell*. 2008; 2:313-319.
2. LIU TM, MARTINA M, HUTMACHER DW et al. Identification of common pathways mediating differentiation of bone marrow- and adipose tissue-derived human mesenchymal stem cells into three mesenchymal lineages. *Stem Cells*. 2007; 25:750-760.
3. RUSSO V, YOUNG S, HAMILTON A et al. Mesenchymal stem cell delivery strategies to promote cardiac regeneration following ischemic injury. *Biomaterials*. 2014; 35:3956-3974.
4. ZHANG W, XUE D, YIN H et al. Overexpression of HSPA1A enhances the osteogenic differentiation of bone marrow mesenchymal stem cells via activation of the Wnt/beta-catenin signaling pathway. *Sci Rep*. 2016; 6:27622.
5. CANCEDDA R, GIANNONI P , MASTROGIACOMO M A tissue engineering approach to bone repair in large animal models and in clinical practice. *Biomaterials*. 2007; 28:4240-4250.
6. CHIU LH, LAI WF, CHANG SF et al. The effect of type II collagen on MSC osteogenic differentiation and bone defect repair. *Biomaterials*. 2014; 35:2680-2691.
7. WANG Q, CHEN B, CAO M et al. Response of MAPK pathway to iron oxide nanoparticles in vitro treatment promotes osteogenic differentiation of hBMSCs. *Biomaterials***.** 2016; 86:11-20.
8. LIU DD, GE K, JIN Y et al. Terbium promotes adhesion and osteogenic differentiation of mesenchymal stem cells via activation of the Smad-dependent TGF-beta/BMP signaling pathway. *J Biol Inorg Chem*. 2014; 19:879-891.
9. SU X, LIAO L, SHUAI Y et al. MiR-26a functions oppositely in osteogenic differentiation of BMSCs and ADSCs depending on distinct activation and roles of Wnt and BMP signaling pathway. *Cell Death Dis*. 2015; 6:e1851.
10. RODRIGUEZ JP, ASTUDILLO P, RIOS S et al. [Adipogenesis and osteoporosis]. *Rev Med Chil*. 2009; 137:827-836.
11. HAASE M, BELLOMO R , HAASE-FIELITZ A Novel biomarkers, oxidative stress, and the role of labile iron toxicity in cardiopulmonary bypass-associated acute kidney injury. *J Am Coll Cardiol*. 2010; 55:2024-2033.
12. ANDREWS NC Iron metabolism: iron deficiency and iron overload. *Annu Rev Genomics Hum Genet*. 2000; 1:75-98.
13. PUNTARULO S Iron, oxidative stress and human health. *Mol Aspects Med*. 2005; 26:299-312.
14. ROSSI F, PERROTTA S, BELLINI G et al. Iron overload causes osteoporosis in thalassemia major patients through interaction with transient receptor potential vanilloid type 1 (TRPV1) channels. *Haematologica*. 2014; 99:1876-1884.
15. TSAY J, YANG Z, ROSS FP et al. Bone loss caused by iron overload in a murine model: importance of oxidative stress. *Blood*. 2010; 116:2582-2589.
16. VOGIATZI MG, MACKLIN EA, FUNG EB et al. Bone disease in thalassemia: a frequent and still unresolved problem. *J Bone Miner Res*. 2009; 24:543-557.

17. GUGGENBUHL P, DEUGNIER Y, BOISDET JF et al. Bone mineral density in men with genetic hemochromatosis and HFE gene mutation. *Osteoporos Int*. 2005; 16:1809-1814.
18. SCHROECK JL, FORD J, CONWAY EL et al. Review of Safety and Efficacy of Sleep Medicines in Older Adults. *Clin Ther*. 2016; 38:2340-2372.
19. PESCHKE E, BAHR I , MUHLBAUER E Experimental and clinical aspects of melatonin and clock genes in diabetes. *J Pineal Res*. 2015; 59:1-23.
20. FAREZ MF, CALANDRI IL, CORREALE J et al. Anti-inflammatory effects of melatonin in multiple sclerosis. *Bioessays*. 2016; 38:1016-1026.
21. REITER RJ, MAYO JC, TAN DX et al. Melatonin as an antioxidant: under promises but over delivers. *J Pineal Res*. 2016; 61:253-278.
22. MANCHESTER LC, COTO-MONTES A, BOGA JA et al. Melatonin: an ancient molecule that makes oxygen metabolically tolerable. *J Pineal Res*. 2015; 59:403-419.
23. JUNG-HYNES B, REITER RJ , AHMAD N Sirtuins, melatonin and circadian rhythms: building a bridge between aging and cancer. *J Pineal Res*. 2010; 48:9-19.
24. OLCESE JM, CAO C, MORI T et al. Protection against cognitive deficits and markers of neurodegeneration by long-term oral administration of melatonin in a transgenic model of Alzheimer disease. *J Pineal Res*. 2009; 47:82-96.
25. BONNEFOND A, CLEMENT N, FAWCETT K et al. Rare MTNR1B variants impairing melatonin receptor 1B function contribute to type 2 diabetes. *Nat Genet*. 2012; 44:297-301.
26. AMSTRUP AK, SIKJAER T, HEICKENDORFF L et al. Melatonin improves bone mineral density at the femoral neck in postmenopausal women with osteopenia: a randomized controlled trial. *J Pineal Res*. 2015; 59:221-229.
27. MARIA S , WITT-ENDERBY PA Melatonin effects on bone: potential use for the prevention and treatment for osteopenia, osteoporosis, and periodontal disease and for use in bone-grafting procedures. *J Pineal Res*. 2014; 56:115-125.
28. ZHANG L, SU P, XU C et al. Melatonin inhibits adipogenesis and enhances osteogenesis of human mesenchymal stem cells by suppressing PPARgamma expression and enhancing Runx2 expression. *J Pineal Res*. 2010; 49:364-372.
29. NAKADE O, KOYAMA H, ARIJI H et al. Melatonin stimulates proliferation and type I collagen synthesis in human bone cells in vitro. *J Pineal Res*. 1999; 27:106-110.
30. LADIZESKY MG, BOGGIO V, ALBORNOZ LE et al. Melatonin increases oestradiol-induced bone formation in ovariectomized rats. *J Pineal Res*. 2003; 34:143-151.
31. PEI M, HE F , KISH VL Expansion on extracellular matrix deposited by human bone marrow stromal cells facilitates stem cell proliferation and tissue-specific lineage potential. *Tissue Eng Part A*. 2011; 17:3067-3076.
32. CAI B, TAN X, ZHANG Y et al. Mesenchymal Stem Cells and Cardiomyocytes Interplay to Prevent Myocardial Hypertrophy. *Stem Cells Transl Med*. 2015; 4:1425-1435.
33. NADERI-MESHKIN H, BAHRAMI AR, BIDKHORI HR et al. Strategies to improve homing of mesenchymal stem cells for greater efficacy in stem cell therapy. *Cell Biol*

Int. 2015; 39:23-34.
34. DANJOU F, ORIGA R, ANNI F et al. Longitudinal analysis of heart and liver iron in thalassemia major patients according to chelation treatment. *Blood Cells Mol Dis*. 2013; 51:142-145.
35. SUZUKI T, TOMONAGA M, MIYAZAKI Y et al. Japanese epidemiological survey with consensus statement on Japanese guidelines for treatment of iron overload in bone marrow failure syndromes. *Int J Hematol*. 2008; 88:30-35.
36. LI GF, PAN YZ, SIROIS P et al. Iron homeostasis in osteoporosis and its clinical implications. *Osteoporos Int*. 2012; 23:2403-2408.
37. KARBOWNIK M , REITER RJ Antioxidative effects of melatonin in protection against cellular damage caused by ionizing radiation. *Proc Soc Exp Biol Med*. 2000; 225:9-22.
38. CHAI X, LI D, CAO X et al. Corrigendum: ROS-mediated iron overload injures the hematopoiesis of bone marrow by damaging hematopoietic stem/progenitor cells in mice. *Sci Rep*. 2017; 7:41900.

Melatonin protects bone marrow mesenchymal stem cells against iron overload-induced osteogenic differentiation dysfunction and senescence

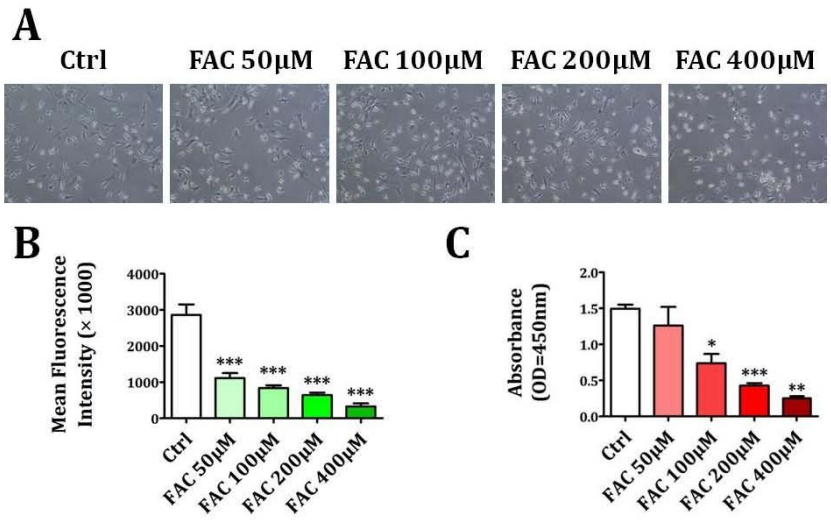

FIGURE 1 FAC-induced iron overload caused the decrease of cell viability in BMSCs. (A) BMSCs exposed to FAC showed fibroblastic morphological changes and reduced cell density compared to the cells without FAC treatment. Moreover, treatment with FAC 400 μM resulted in cell floating and death on most of BMSCs; (B) Labile iron pool (LIP) assay showed that exposure to FAC 50 μM, 100 μM, 200 μM and 400 μM caused concentration-dependent iron overload in BMSCs; (C) CCK-8 assay showed that Mel played a significant protective role in the cellular viability of BMSCs in a dose-dependent manner for 24 h. Values are the mean ± SEM of 3 independent experiments ($n = 3$). * $p < 0.05$, ** $p < 0.01$, *** $p < 0.001$.

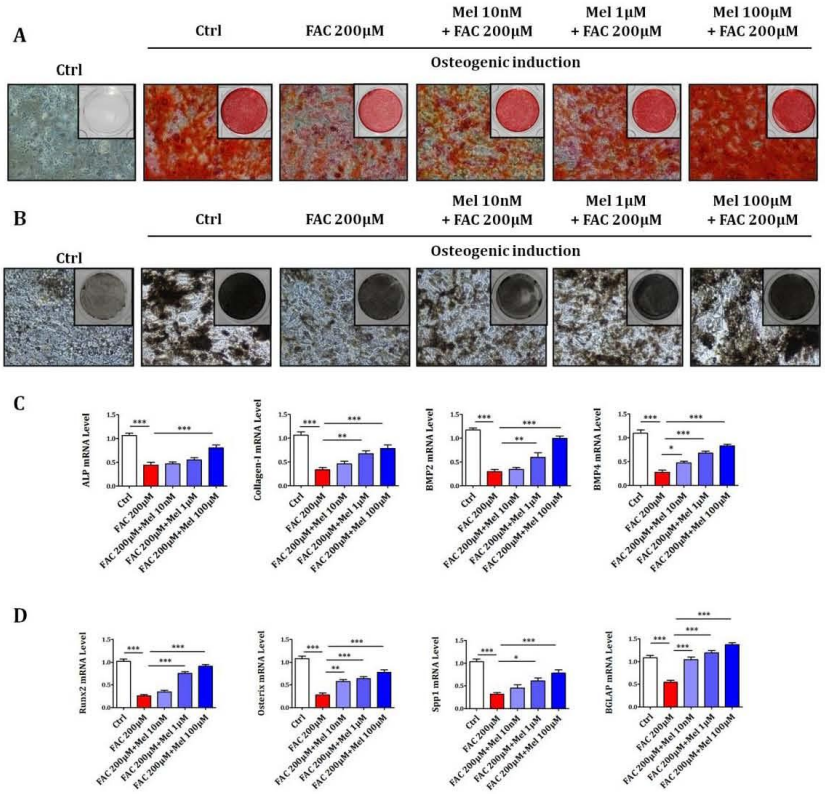

FIGURE 2 Melatonin protected BMSCs against FAC-induced inhibition of osteogenic differentiation. (A-B) ARS and ALP staining were used to evaluate the osteogenic differentiation ability of different concentrations of melatonin in FAC-induced BMSCs. Results showed that FAC-induced iron overload markedly inhibited the differentiation of BMSCs into osteoblast lineage. However, melatonin-treated BMSCs showed a concentration-dependent increase of mineralized areas from 10 nM to 100 μM melatonin treatment; (C-D) The transcription levels of osteoblast-specific genes (ALP, Collagen-I, BMP2 and BMP4) and osteogenic transcription factors (Runx2, Osterix, Spp1 and BGLAP) were examined by qRT-PCR

to evaluate the osteogenic differentiation ability of melatonin in FAC-induced BMSCs. qRT-PCR assay showed that these factors involved in the osteogenic differentiation decreased after exposure to FAC 200 μM, but treatment with melatonin 10 nM, 1 μM and 100 μM increased the mRNA levels. Values are the mean ± SEM of 3 independent experiments ($n = 3$). * $p < 0.05$, ** $p < 0.01$, *** $p < 0.001$.

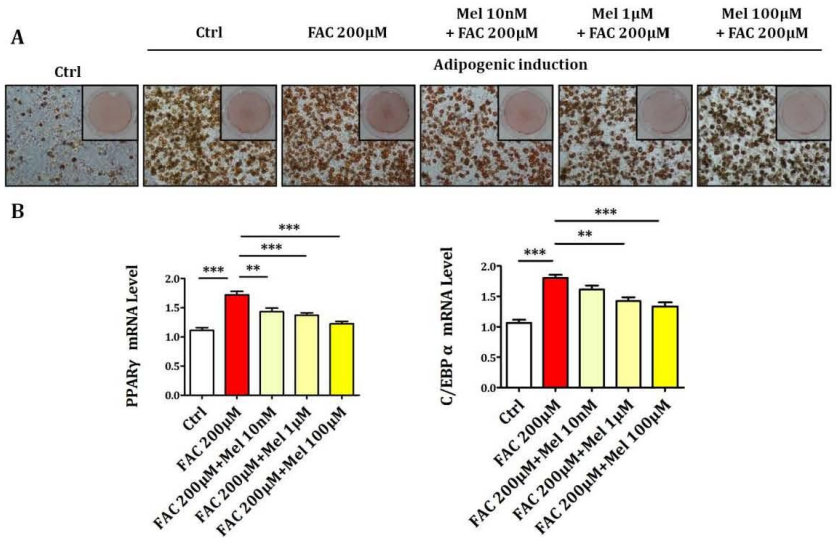

FIGURE 3 Melatonin prevented adipogenic differentiation of BMSCs in response to FAC. (A) Oil red O staining results showed that FAC-induced iron overload promoted the differentiation of BMSCs into adipogenic lineage. But, melatonin-treated BMSCs showed a decrease quantity of red oil drops ranging from melatonin 10 nM to 100 μM; (B) Transcription levels of adipogenic-specific genes including PPARγ and C/EBPα were examined by qRT-PCR. Results showed that exposure to FAC 200 μM increased the expression of adipogenic-specific genes PPARγ and C/EBPα compared to control group, which was partially reversed by melatonin 10 nM, 1 μM and 100 μM. Values are the mean ± SEM of 3 independent experiments (n = 3). ** $p < 0.01$, *** $p < 0.001$.

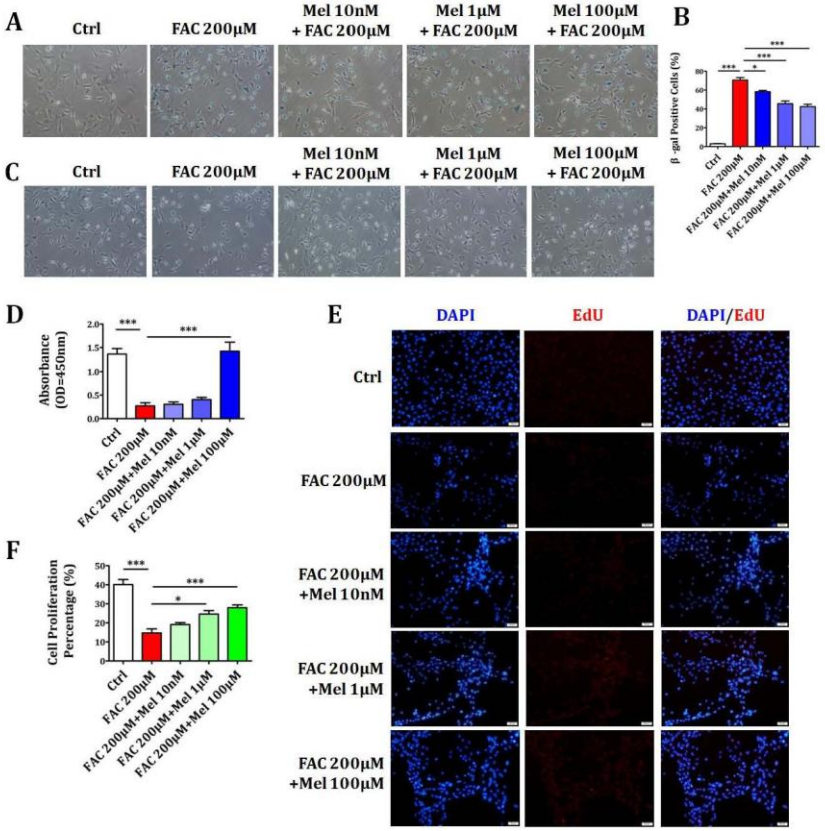

FIGURE 4 Effects of melatonin on FAC-induced proliferation reduction and senescence of BMSCs. (A-B) β-gal staining showed that a significant increase of β-gal-positive cells was observed in the FAC-treated BMSCs, while treatment with melatonin at 10 nM, 1 μM and 100 μM could significantly decrease the percentage of β-gal-positive senescent BMSCs to varying degrees respectively; (C) Morphological observation revealed that exposed to FAC 200 μM resulted in a significant morphological destruction in BMSCs compared to control group, while this alteration was remarkably attenuated in the presence of different concentrations of melatonin treatment; (D) CCK-8 assay result confirmed that cell viability was significantly

inhibited by FAC 200 μM treatment, while melatonin treatment induced a gradual increase of viability of BMSCs at concentrations ranging from 10 nM to 100 μM; (E-F) EdU assay results proved that BMSCs exhibited less EdU-positive staining compared to control group when treated with FAC 200 μM for 24 h. However, in the presence of different concentrations of melatonin, BMSCs showed a concentration-dependent increase of EdU-positive staining compared to the FAC group. Values are the mean ± SEM of 3 independent experiments ($n = 3$). * $p < 0.05$, *** $p < 0.001$.

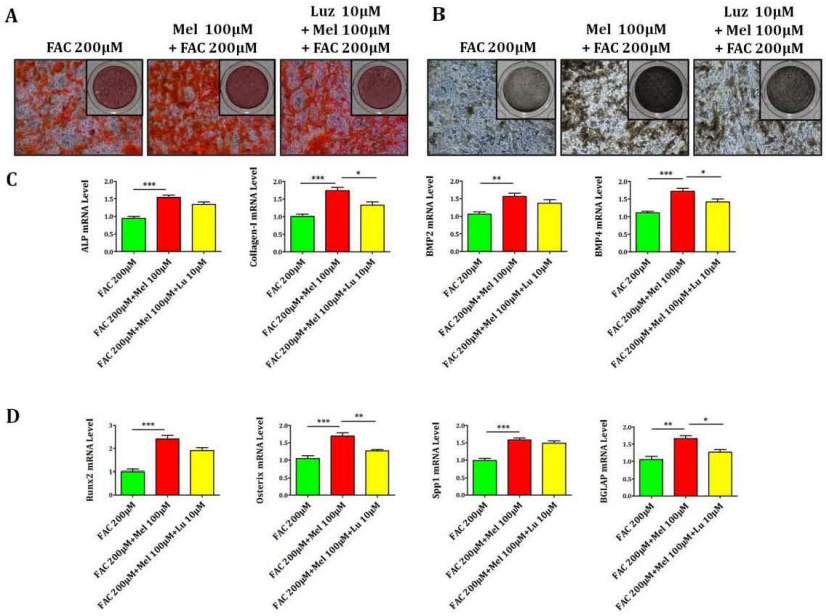

FIGURE 5 Effect of melatonin inhibitor luzindole on FAC-induced osteogenic differentiation of BMSCs. (A-B) ARS staining and ALP staining showed that luzindole treatment blocked melatonin-induced the increase of mineralized areas in FAC-treated BMSCs; (C-D) The transcription levels of osteoblast-specific genes (ALP, Collagen-I, BMP2 and BMP4) and osteogenic transcription factors (Runx2, Osterix, Spp1 and BGLAP) were examined by qRT-PCR to evaluate the osteogenic differentiation ability of luzindole and melatonin in FAC-induced BMSCs. qRT-PCR results showed that luzindole abolished melatonin-induced upregulation of osteoblast-specific genes and osteogenic transcription factors in FAC-treated BMSCs. Values are the mean ± SEM of 3 independent experiments ($n = 3$). * $p < 0.05$, ** $p < 0.01$, *** $p < 0.001$.

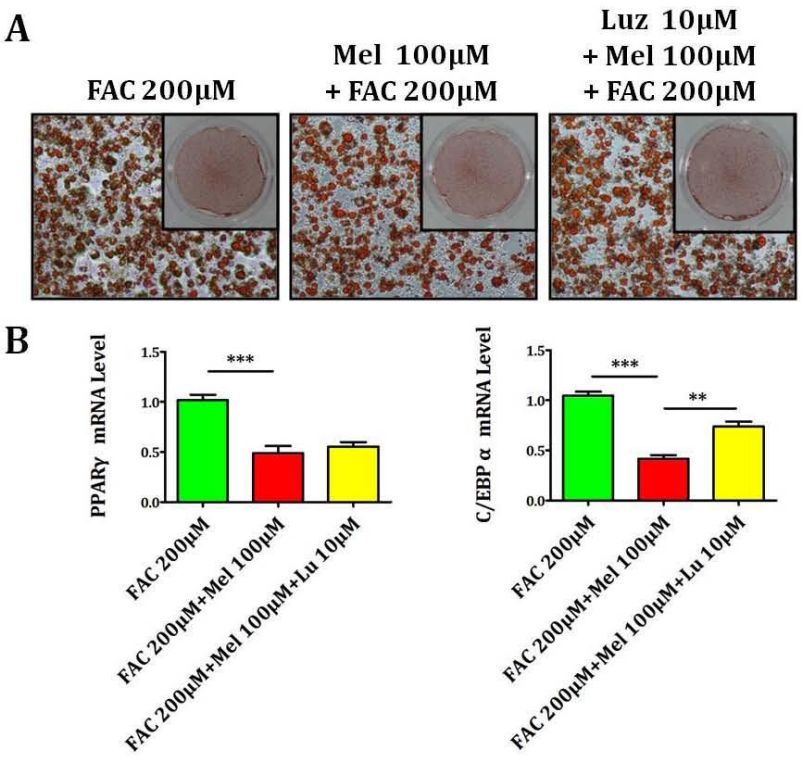

FIGURE 6 Effect of melatonin inhibitor luzindole on FAC-induced adipogenic differentiation of BMSCs. (A) Oil red O staining showed that melatonin-induced the decrease of red oil drops in FAC-induced BMSCs was reversed by luzindole 10 μM supplementation; (B) qRT-PCR results showed that luzindole abolished melatonin-induced downregulation of adipogenic-specific genes PPARγ and C/EBPα in FAC-treated BMSCs. Values are the mean ± SEM of 3 independent experiments (n = 3). ** $p < 0.01$, *** $p < 0.001$.

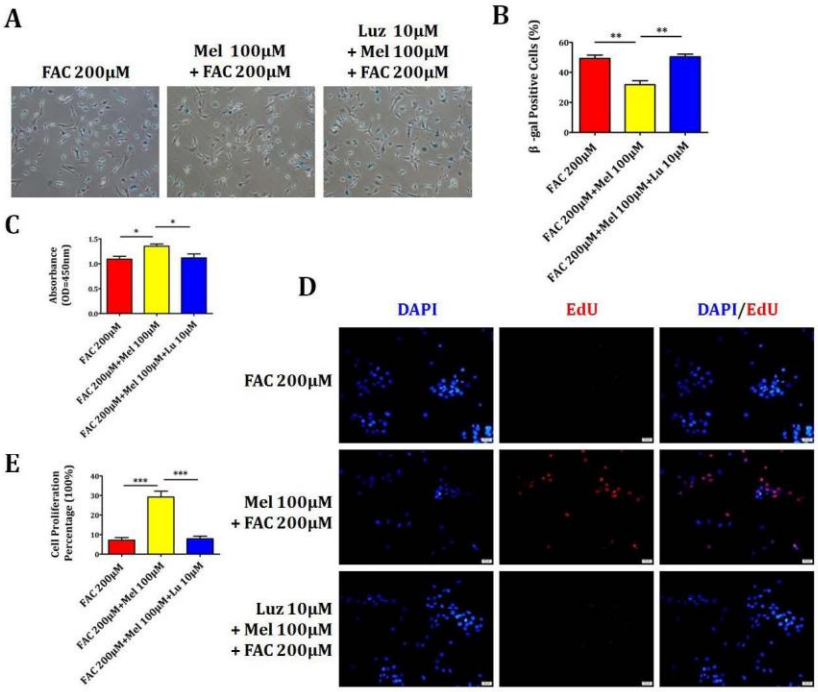

FIGURE 7 Melatonin inhibitor luzindole abolished FAC-induced proliferation reduction and senesence of BMSCs. (A-B) β-gal staining showed that melatonin 100 μM inhibited the β-gal-positive senescent BMSCs compared to the FAC 200 μM group, which could be also reversed by luzindole 10 μM; (C) CCK-8 result showed that melatonin 100 μM significantly attenuated FAC-induced the decrease of viability of BMSCs, but this improvement could be markedly blocked by melatonin inhibitor luzindole 10 μM; (D-E) EdU assay result showed that melatonin 100 μM could improve the proliferation of FAC-treated BMSCs, but in the presence of luzindole 10 μM, melatonin fail to ameliorate FAC-induced proliferation reduction of BMSCs. Values are the mean ± SEM of 3 independent experiments (n = 3). * $p < 0.05$, ** $p < 0.01$, *** $p < 0.001$.

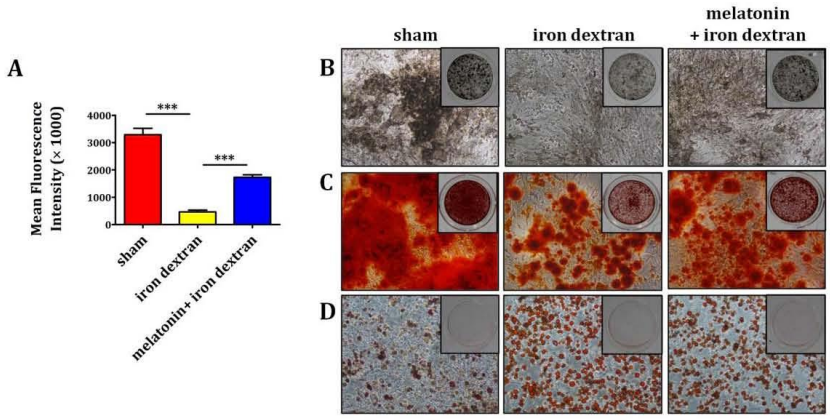

FIGURE 8 Melatonin prevented iron dextran-induced inhibition of osteogenic differentiation and promotion of adipogenic differentiation in vivo. (A) LIP was tested by flow cytometry to confirm the establishment of iron overload mouse model; (B-C) ARS staining and ALP staining were used to evaluate the osteogenic differentiation ability of melatonin in iron dextran-induced iron overload of BMSCs. Stainings showed that iron dextran-induced iron overload markedly inhibited differentiation of BMSCs into osteoblast lineage. However, melatonin-treated BMSCs showed an increase of mineralized areas; (D) Oil red O staining results showed that iron dextran-induced iron overload promoted the differentiation of BMSCs into adipogenic lineage. But, melatonin cotreatment on BMSCs showed a decrease quantity of red oil drops. Values are the mean ± SEM of 3 independent experiments (n = 3). *** $p <$ 0.001.

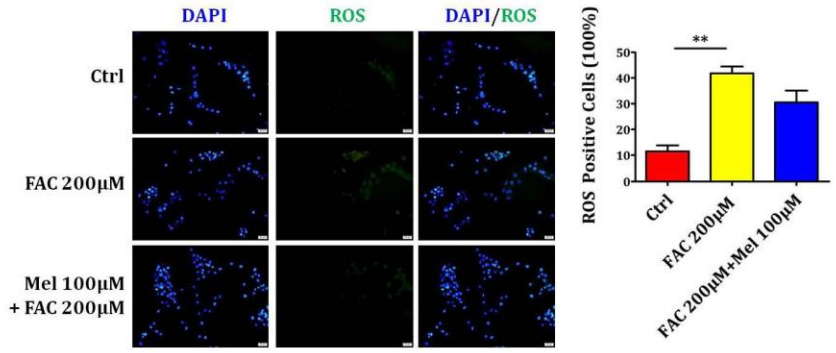

FIGURE 9 Melatonin reversed FAC-induced increase of ROS in BMSCs. DCFH-DA probe was applied to evaluate the effect of luzindole and melatonin on the production of intracelluar ROS in FAC-induced BMSCs. Results showed that intracellular ROS level was increased in the presence of FAC 200 μM for 24 h, which was reversed by treatment with melatonin 100 μM. Values are the mean ± SEM of 3 independent experiments ($n = 3$). ** $p < 0.01$.

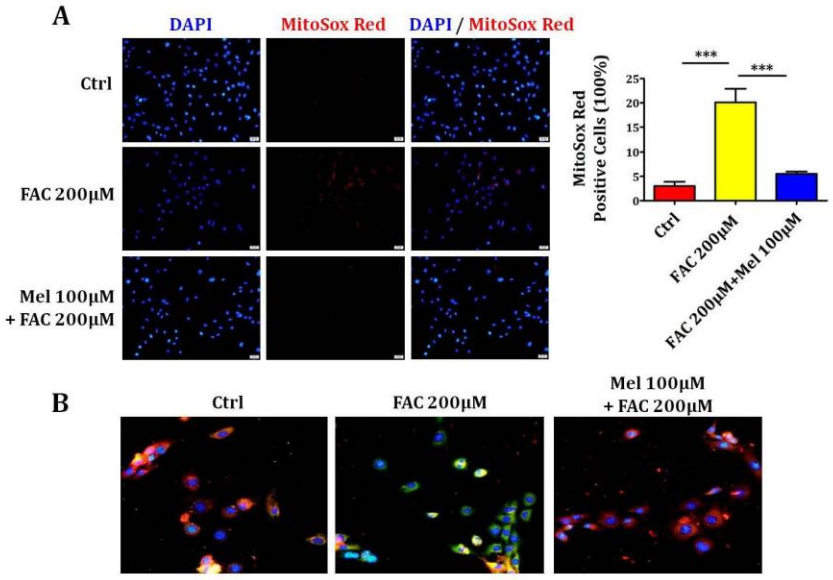

FIGURE 10 Melatonin reversed FAC-induced mitochondrial dysfunction in BMSCs. (A) Superoxide production in the mitochondria was measured using MitoSOX™ Red assay. Treatment of BMSCs with FAC 200 μM for 24 h led to an increase of mitochondrial superoxide productions manifested by the increasing red fluorescence, while the red fluorescence could be inhibited by treatment with melatonin 100 μM; (B) The JC-1 probe detection result showed that treatment of BMSCs with FAC 200 μM for 24 h caused the loss of mitochondrial membrane potential, which could be ameliorated by treatment with melatonin 100 μM. Values are the mean ± SEM of 3 independent experiments ($n = 3$). *** $p < 0.001$.

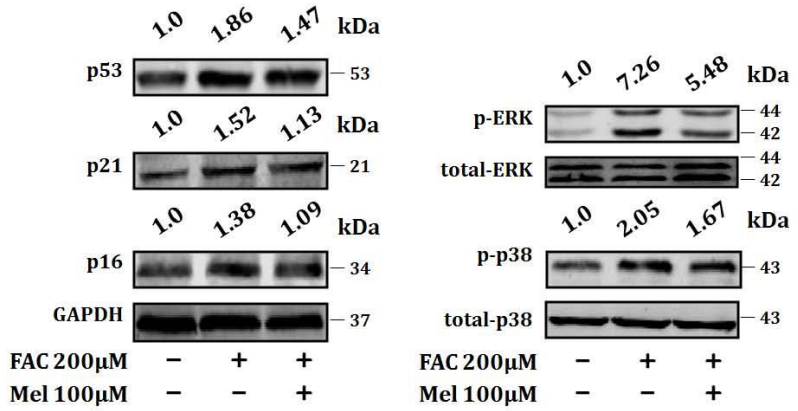

FIGURE 11 Melatonin suppressed FAC-induced BMSCs injury by blocking p53/ERK/p38 signal pathway. Western blot results showed that the protein expression levels of p53, p21, p16, phosphorylated and total protein levels of ERK and p38 significantly increased in FAC-treatment groups compared to the control group. While, in the presence of melatonin 100 μM, melatonin ameliorated the increased the protein expressions of p53, p21 and p16, as well as phosphorylated and total ERK and p38 in FAC-treated BMSCs. Values are the mean ± SEM of 3 independent experiments (n = 3).